Human Arginase II: Crystal Structure and Physiological Role in Male and Female Sexual Arousal[†,‡]

Evis Cama,[§] Diana M. Colleluori,[||,⊥] Frances A. Emig,[||] Hyunshun Shin,[§] Soo Woong Kim,[#] Noel N. Kim,[#] Abdulmaged M. Traish,[#] David E. Ash,[||] and David W. Christianson*[,§]

Roy and Diana Vagelos Laboratories, Department of Chemistry, University of Pennsylvania, Philadelphia, Pennsylvania 19104-6323, Department of Biochemistry, Temple University School of Medicine, Philadelphia, Pennsylvania 19140, and Departments of Urology and Biochemistry, Boston University School of Medicine, 700 Albany Street, Boston, Massachusetts 02118

Received February 28, 2003; Revised Manuscript Received May 21, 2003

ABSTRACT: Arginase is a binuclear manganese metalloenzyme that catalyzes the hydrolysis of L-arginine to form L-ornithine and urea. The X-ray crystal structure of a fully active, truncated form of human arginase II complexed with a boronic acid transition state analogue inhibitor has been determined at 2.7 Å resolution. This structure is consistent with the hydrolysis of L-arginine through a metal-activated hydroxide mechanism. Given that human arginase II appears to play a role in regulating L-arginine bioavailability to NO synthase in human penile corpus cavernosum smooth muscle, the inhibition of human arginase II is a potential new strategy for the treatment of erectile dysfunction [Kim, N. N., Cox, J. D., Baggio, R. F., Emig, F. A., Mistry, S., Harper, S. L., Speicher, D. W., Morris, S. M., Ash, D. E., Traish, A. M., and Christianson, D. W. (2001) *Biochemistry 40,* 2678−2688]. Since NO synthase is found in human clitoral corpus cavernosum and vagina, we hypothesized that human arginase II is similarly present in these tissues and functions to regulate L-arginine bioavailability to NO synthase. Accordingly, hemodynamic studies conducted with a boronic acid arginase inhibitor in vivo are summarized, suggesting that the extrahepatic arginase plays a role in both male and female sexual arousal. Therefore, arginase II is a potential target for the treatment of male and female sexual arousal disorders.

Arginase is a binuclear manganese metalloenzyme that catalyzes the hydrolysis of L-arginine to form L-ornithine and urea through a metal-activated hydroxide mechanism (Figure 1a) (*1*, *2*). In mammals, two isozymes are identified: arginase I is found predominantly in hepatocytes where it catalyzes the final cytosolic step of the urea cycle (*3*), and arginase II is extrahepatic (e.g., kidneys, small intestine, lactating mammary gland, penile corpus cavernosum) (*3*−*6*) and localizes subcellularly in the mitochondrial matrix of kidney cells (*7*). Arginase isozymes differ from each other in terms of their catalytic, molecular, and immunological properties. Unlike arginase I, the primary function of arginase II appears to be in L-arginine homeostasis (*8*−*10*), regulating L-arginine or L-ornithine pools for subsequent biosynthetic transformations (*11*).

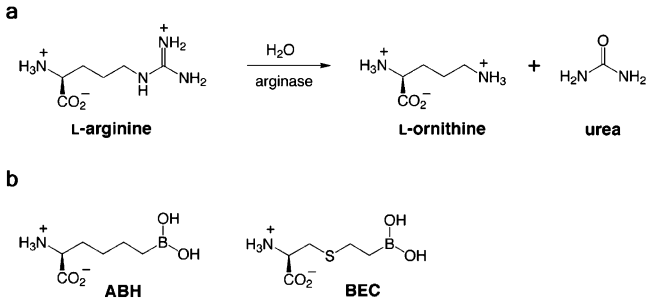

FIGURE 1: (a) Arginase reaction. (b) Arginase inhibitors 2(*S*)-amino-6-boronohexanoic acid (ABH) and *S*-(2-boronoethyl)-L-cysteine (BEC).

Being the predominant extrahepatic isozyme, arginase II can play a key role in the regulation of L-arginine bioavailability to NO synthase, given that both enzymes compete for the same substrate, L-arginine. In principle, arginase activity should attenuate NO biosynthesis and NO-dependent processes by attenuating L-arginine bioavailability to NO synthase, and arginase inhibition should enhance NO biosynthesis and NO-dependent processes by enhancing L-arginine bioavailability to NO synthase. Accordingly, recent studies demonstrate that potent boronic acid inhibitors of arginase enhance NO-dependent smooth muscle relaxation in rabbit and human penile corpus cavernosum (*6*, *12*). Additionally, the gene expression, protein level, and catalytic activity of arginase II are elevated in diabetic corpus

[†] This work was supported by National Institutes of Health Grants GM49758 (D.W.C.), GM67788 (D.E.A.), DK02696 (N.N.K.), and DK56846 (A.M.T.). E.C. was supported in part by the U.S. Army Medical Research and Materiel Command's Office of the Congressionally Directed Medical Research Programs through a Department of Defense Breast Cancer Research Predoctoral Fellowship.

[‡] The atomic coordinates for human arginase II complexed with *S*-(2-boronoethyl)-L-cysteine have been deposited in the Protein Data Bank, www.rcsb.org, with accession code 1PQ3.

* To whom correspondence should be addressed. E-mail: chris@xtal.chem.upenn.edu.

[§] University of Pennsylvania.

[||] Temple University.

[⊥] Current address: Institute for Cancer Research, Fox Chase Cancer Center, Philadelphia, PA 19111.

[#] Boston University.

10.1021/bi034340j CCC: $25.00
Published on Web 06/26/2003

cavernosum, and NO biosynthesis is enhanced by treatment with a boronic acid inhibitor of arginase (*13*).

The cDNA of human arginase II has been isolated and characterized and encodes a 354-residue protein, including a putative, 22-residue N-terminal mitochondrial targeting sequence (*14*, *15*). The deduced amino acid sequence of human arginase II is 62% identical to that of rat arginase I and 60% identical to that of human arginase I; all active site residues implicated in catalysis, including the metal ligands, are strictly conserved. Mature human arginase II exists predominantly as a 129 kDa trimer (*16*), which is larger than the 105 kDa trimer of rat arginase I (*17*). Mature human arginase II contains one inserted residue, 85A, in the loop between helices B1 and B2 and 12 additional residues at the C-terminus. The K_M of L-arginine for human arginase II is approximately 4.8 mM at physiological pH (*16*), which is not significantly different from the K_M of 1.4 mM measured for rat arginase I (*18*). Amino acid inhibitors with modest isozyme selectivity have been identified (Figure 1b): 2(*S*)-amino-6-boronohexanoic acid (ABH) and *S*-(2-boronoethyl)-L-cysteine (BEC) bind tightly to rat arginase I at pH 8.5 with K_d values of 0.11 and 2.2 μM, respectively, measured by isothermal titration calorimetry (*6*, *20*) and are potent inhibitors of human arginase II at pH 9.5 with K_i values of 8.5 and 30 nM, respectively, measured by kinetic assay (*19*).

Here, we report the X-ray crystal structure of a fully active, truncated form of human arginase II complexed with the inhibitor BEC at 2.7 Å resolution. The truncation variant is ΔM1-V23/ΔH331-I354 (114 kDa trimer), which was constructed to circumvent aggregation problems observed with the wild-type enzyme (*16*). The arginase II−BEC structure provides important insights regarding structure−affinity relationships for inhibitors binding to human arginase II and rat arginase I (*21*). Importantly, arginase II−BEC complexation causes 20−50% enhanced NO-dependent relaxation of penile corpus cavernosum smooth muscle in electrophysiological organ bath experiments, suggesting that arginase inhibition may enhance male erectile function (*6*). Given that NO synthase is identified in human clitoral corpus cavernosum (*22*) and vagina (*23*), arginase II may also colocalize in these tissues; if so, an arginase inhibitor may similarly enhance smooth muscle relaxation and female sexual arousal. Accordingly, we report the results of hemodynamic experiments conducted in vivo that suggest a role for arginase II in regulating both male and female sexual arousal.

MATERIALS AND METHODS

Arginase Inhibitors. The arginase inhibitor ABH was synthesized with some modifications to published procedures (*24*). Briefly, (*S*)-1-*tert*-butyl-2-[bis-(*tert*-butoxycarbonyl)-amino]-5-hexenoate was prepared (*25*) from the commercially available L-glutamic acid derivative for hydroboration, followed by treatment with methanol to quench unreacted borane and protected with (1*S*, 2*S*, 3*R*, 5*S*)-(+)-pinanediol (*26*, *27*). Complete deprotection with BCl_3 yielded ABH (*24*, *28*). The arginase inhibitor BEC was purchased from QVentas (Newark, DE).

Expression, Purification, and Assay of Truncated Human Arginase II. The ΔM1-V23/ΔH331-I354 variant of human arginase II was constructed by site-directed mutagenesis and transformation using the QuikChange Site-Directed Mutagenesis Kit (Stratagene) using mature human arginase II cDNA (*16*). The following primers were used to generate the variant: sense mutagenic primer, CAGACAAGAGAAG-GAGGGCATTAGGTCTATGACCAACTTCCTACTCCC and antisense mutagenic primer, GGGAGTAGGAAGTTG-GTCATAGACCTAATGCC CTCCTTCTCTTGTCTG (mutated codons are underlined). The variant was expressed in *Escherichia coli* BL21(DE3) as described for the wild-type enzyme (*16*). The purification protocol for the variant was the same as that reported for the wild-type enzyme (*16*), with a minor modification: following DEAE chromatography and concentration using Millipore centrifugal filters, the variant was precipitated with ammonium sulfate from a 50 mM HEPES-KOH (pH 7.5) solution and centrifuged. The resultant pellet was resolubilized in 50 mM HEPES-KOH (pH 7.5). Arginase activity was assayed as described (*16*).

Crystallography. Crystallization was performed at 4 °C by the hanging drop vapor diffusion method. Drops containing 3 μL of 7 mg/mL human arginase II, 5 mM BEC, 50 mM bicine (pH 8.5), and 100 μL of $MnCl_2$ were mixed with 3 μL of precipitant buffer (0.10 M Tris-HCl (pH 8.3−8.5), 3.0 M $(NH_4)_2SO_4$) and equilibrated over a 1 mL reservoir of 0.10 M Tris-HCl (pH 8.3−8.5), 3.0 M $(NH_4)_2SO_4$, 20% (v/v) glycerol. X-ray diffraction data to 2.7 Å resolution were collected from a single flash-cooled crystal of the arginase II−BEC complex at the Cornell High Energy Synchrotron Source (beamline F-1), and intensity data integration and reduction were performed using DENZO and SCALEPACK, respectively (*29*). Crystals belong to space group $P3_2$ with unit cell dimensions $a = 142.99$ Å, $b = 142.99$ Å, and $c = 127.32$ Å, with two trimers in the asymmetric unit.

Initial phases were determined by molecular replacement with AMoRe (*30*, *31*) using the structure of the native rat liver arginase trimer (*21*) as a search probe. Using intensity data in the 20−3 Å shell, a cross rotation search yielded two peaks with correlation coefficients of 14.1. Subsequent translation searches using these two highest peaks produced two solutions with correlation coefficients of 16.1. Rigid body refinement with these solutions yielded $R = 0.494$. Iterative rounds of model building and refinement were performed using O (*32*) and CNS (*33*), respectively. The final structure contains 407 water molecules and 15 sulfate anions. In the final stages of refinement, the inhibitor BEC was built into clear and unbiased electron density, and the complex was refined to convergence with $R = 0.227$ ($R_{free} = 0.247$). Data collection and refinement statistics are reported in Table 1.

Tissue Arginase Activity Measurements. Rabbit vaginal tissue was divided into proximal and distal segments, frozen in liquid nitrogen, and pulverized. The tissue powder was homogenized 1:4 (wt/vol) at 4 °C in 20 mM HEPES (pH 7.4), 0.25 M sucrose containing mammalian protease inhibitor cocktail (Sigma-Aldrich Co., St. Louis, MO). The homogenate was centrifuged at 3000*g* for 20 min at 4 °C, and the resulting supernatant was used to determine arginase activity, as previously described (*6*).

Hemodynamic Studies of Male and Female Genitalia in Vivo. All protocols were approved by the Institutional Animal Care and Use Committee at the Boston University School of Medicine. Male and female New Zealand White rabbits (4.0−4.5 kg) were anesthetized with ketamine (35 mg/kg) and xylazine (5 mg/kg). Systemic blood pressure was

Table 1: Data Collection and Refinement Statistics

resolution (Å)	2.7	R_{cryst}[d]	0.227
total reflections (*N*)	404391	R_{free}[d]	0.247
unique reflections (*N*)	79653	rms deviations	
completeness (%) (last shell)	99.3 (98.9)[a]	bonds (Å)	0.007
R_{merge} (last shell)[b]	0.098 (0.280)[a]	angles (deg)	1.4
reflections used in refinement (test set)	75977 (3837)	dihedrals (deg)	24.0
sulfate anions[c]	15	impropers (deg)	1.0
solvent atoms (N)[c]	407		

[a] Numbers in parentheses refer to the outer 0.1 Å shell of data. [b] R_{merge} for replicate reflections, $R = \sum|I_h - \langle I_h \rangle|/\sum\langle I_h \rangle$; I_h = intensity measured for reflection *h* and $\langle I_h \rangle$ = average intensity for reflection *h* calculated from replicate data. [c] Per asymmetric unit. [d] Crystallographic *R* factor, $R_{cryst} = \sum||F_o| - |F_c||/\sum|F_o|$ for reflections contained in the working set. Free *R* factor, $R_{free} = \sum||F_o| - |F_c||/\sum|F_o|$ for reflections contained in the test set held aside during refinement (5% of total). $|F_o|$ and $|F_c|$ are the observed and calculated structure factor amplitudes, respectively.

continuously recorded by means of a 20-gauge angiocatheter inserted into the carotid artery and connected to a PT300 pressure transducer (Grass Instruments/Astro-Med, Inc., Warwick, RI). A bipolar platinum wire electrode was applied to the pelvic nerve, and unilateral pelvic nerve stimulation was accomplished with a 30 s train of square waves with 10 V pulse amplitude and 0.8 ms pulse duration. Stimulation frequency was 8 Hz in male and 2 Hz in female rabbits. These parameters have been previously determined to result in submaximal responses.

For assessment of penile erectile function in male rabbits, a 23-gauge needle with PE-50 tubing was filled with normal saline containing 50 U/mL heparin and inserted into one of the cavernosal bodies of the penis. The line was then attached to a PT300 pressure transducer, and intracavernosal pressure was recorded by means of a PI-1-ACDC signal conditioner module and a Grass 7400 physiological recorder (Grass Instruments Div., Astro-Med, Inc., Warwick, RI).

For assessment of genital engorgement in female rabbits, a dual channel laser oximeter (Model 96208; ISS, Inc., Champaign, IL) was utilized, as described previously (*34*). The skin around the labia was shaved to ensure good contact with the optical fibers. The probe was positioned longitudinally, externally over the clitoris, labia, and lower vagina such that the detector fiber was positioned just below the pubic arch. The changes in the concentration of oxyhemoglogin were used as parameters reflecting changes in genital blood flow.

Control responses to pelvic nerve stimulation were determined in rabbits after intracavernosal (male; 0.15 mL) or intravenous (female; 1 mL) administration of vehicle (40% propylene glycol). After 20 min, ABH was administered, and pelvic nerve stimulation was repeated 10 min after drug infusion. The dose of ABH was 150 μg in male rabbits (intracavernosal) and 4 or 6 mg/kg in female rabbits (intravenous).

The amplitude, duration, and area-under-the-curve was determined for each response, and data were expressed as mean ± SEM. For intracavernosal pressure measurements, response duration was defined as the time interval between the initial rise in pressure and the return to baseline. For oximetry data, the change in tissue oxyhemoglobin concentration was determined as the difference between baseline and peak amplitude values. Responses to vehicle and ABH were analyzed by a paired *t* test and determined to be significantly different when the *p* value was less than or equal to 0.05.

RESULTS AND DISCUSSION

Activity, Structure, and Mechanistic Inferences. Truncated human arginase II has a k_{cat} value of 203 s^{-1}, comparable to that of 231 s^{-1} measured for the wild-type enzyme; however, the K_M is 2.4 mM, as compared to that of 0.3 mM for the wild-type enzyme at pH 9.5 (*16*). As with the study of BEC binding to arginase I (*6*), analysis of progress curves for the slow binding inhibition of truncated arginase II by BEC indicates a K_i value of 0.23 μM, which is in good agreement with the value of 0.13 μM estimated from the steady-state velocities (see Supporting Information). These K_i values are approximately 4−8-fold greater than the corresponding values measured with full-length wild-type arginase II, so the C-terminus appears to have a minor effect on ligand binding in the arginase II active site. Nevertheless, these K_i values are approximately 10-fold lower than those measured against arginase I (*6*), so truncated human arginase II retains inhibitor selectivity as compared with arginase I.

The polypeptide fold of human arginase II is topologically identical to the α/β fold of rat arginase I (*21*) and the hexameric arginase from *Bacillus caldovelox* (*35*) as expected from the amino acid sequence identities (62 and 39%, respectively) (Figure 2). The rms deviation is 0.64 Å for 305 C_α atoms between human arginase II and rat arginase I and 2.4 Å for 297 C_α atoms between human arginase II and *B. caldovelox* arginase. The greatest structural differences (~9.5 Å) are observed in the H50-V68 segment of the protein that is variable in sequence among the three isozymes (the rat arginase I numbering scheme is adopted for human arginase II).

Monomer−monomer interactions in the trimer are stabilized by an arginine-rich network of intersubunit salt links, sulfate counterions, and hydrogen bonds more extensive than that observed in rat arginase I (*21*), due in part to a greater number of arginine residues located at the subunit interface of human arginase II (Figure 3). Nevertheless, the conserved R308-D204 salt link remains the central feature of these intermolecular interactions. The side chain of R201 (T in rat arginase I) forms an intermonomer salt link with E263 and also hydrogen bonds with water molecules; the side chain of R205 (K in rat arginase I) forms an intermonomer hydrogen bond with N209 (G in rat arginase I) and also hydrogen bonds with water molecules. Sulfate anions salt link with R201 (T in rat arginase I), R205 (K in rat arginase I), R214 (E in rat arginase I), and R223 (K in rat arginase I).

The binuclear manganese cluster of human arginase II is nearly identical to that of rat liver arginase I in its complex with BEC (Figure 4): Mn^{2+}_A is coordinated by D232 (Oδ2), H101 (Nδ1), D128 (Oδ2), D124 (Oδ2), and boronate hydroxyl groups O1 and O2 with distorted octahedral geometry; Mn^{2+}_B is coordinated by H126 (Nδ1), D124 (Oδ1), D234 (Oδ1 and Oδ2), and boronate hydroxyl group O1 with distorted octahedral geometry. Although D232 (Oδ1) coordinates to Mn^{2+}_B in native arginase I (*21*), the side chain moves in the arginase II−BEC complex such that

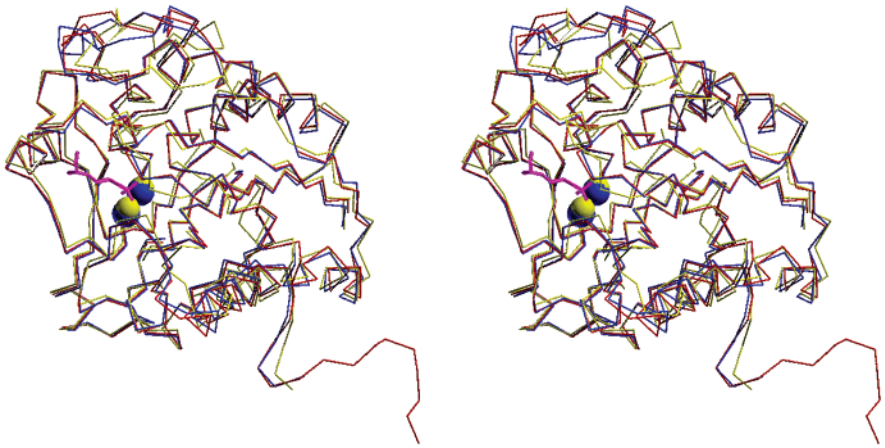

FIGURE 2: Least-squares superposition of monomer C_α traces of rat arginase I (red), human arginase II (blue), and *B. caldovelox* arginase (yellow). Manganese ions appear as spheres; for reference, BEC is shown in magenta.

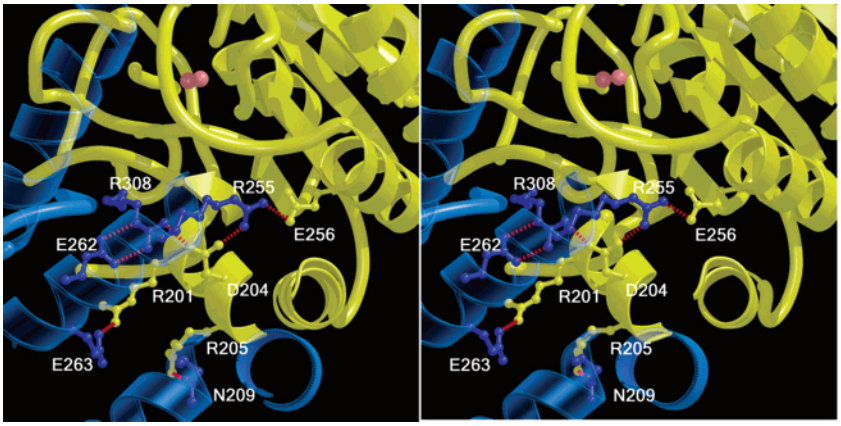

FIGURE 3: Side chains of R201, R205, R255, and R308 nucleate an alternating network of intra- and intersubunit salt-links that stabilize the trimeric quaternary structure. Residues from monomers A and B are blue and yellow, respectively. Manganese ions appear as light-pink spheres. For clarity, intrasubunit hydrogen bonds, water molecules, and sulfate anions are omitted.

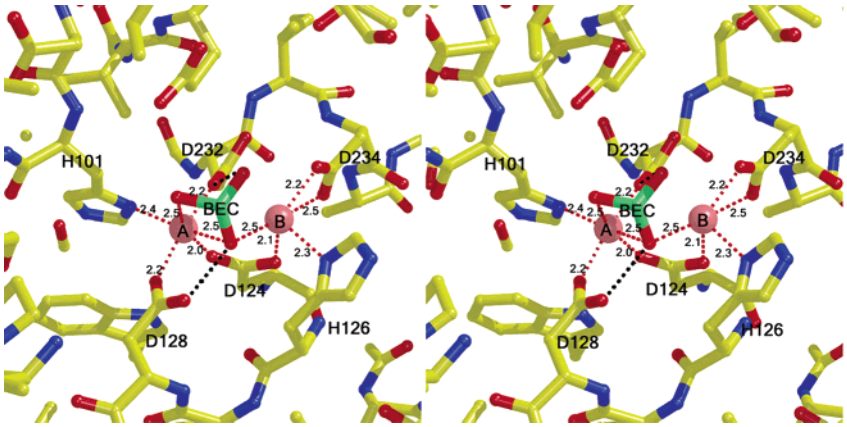

FIGURE 4: Binuclear manganese cluster in the arginase II−BEC complex; for clarity, only the tetrahedral boronate anion of BEC is shown. Atoms are color-coded as follows: C = yellow, O = red, N = blue, S = dark green, and B = pale green; manganese ions appear as light-pink spheres. The corresponding electron density map is found in the Supporting Information.

the D232 (Oδ1)−Mn^{2+}_B separation of 2.6 Å is somewhat long to be considered an inner-sphere coordination interaction. Instead, D232 (Oδ1) is better positioned to accept a hydrogen bond from boronate hydroxyl group O3. Boronate hydroxyl group O1 symmetrically bridges the binuclear manganese cluster, and the Mn^{2+}_A−Mn^{2+}_B separation is 3.3 Å.

An omit electron density map of the arginase II−BEC complex is found in Figure 5. Binding interactions between BEC and the arginase II active site are largely similar, but not identical, to those observed in the arginase I−BEC complex (*6*). The tetrahedral boronate anion of BEC binds in an identical fashion to the binuclear manganese clusters of arginase II and arginase I; additionally, boronate hydroxyl O1 donates a hydrogen bond to D128, and boronate hydroxyl O2 donates a hydrogen bond to the backbone carbonyl of H141. However, boronate hydroxyl O2 donates a hydrogen bond to E277 (O···O separation = 3.0 Å) in the arginase

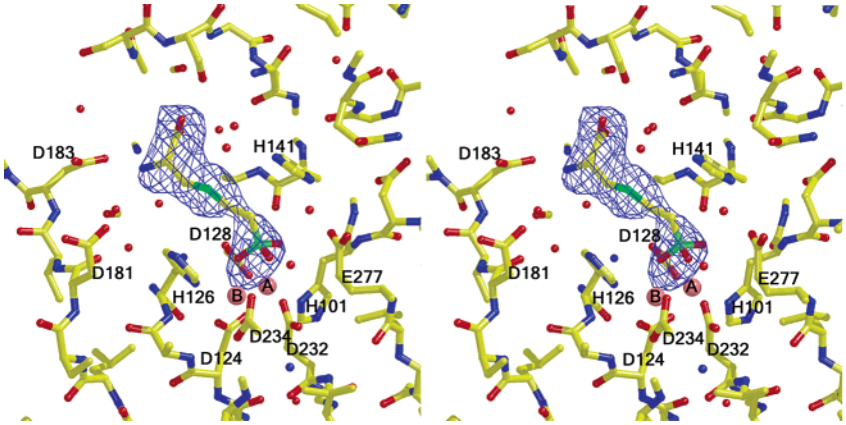

FIGURE 5: Human arginase II−BEC complex. Omit electron density map of BEC in the arginase active site. The map is contoured at 3.8σ, and selected active site residues are indicated. Atoms are color-coded as follows: C = yellow, O = red, N = blue, S = dark green, and B = pale green; manganese ions appear as light-pink spheres, and water molecules appear as red spheres.

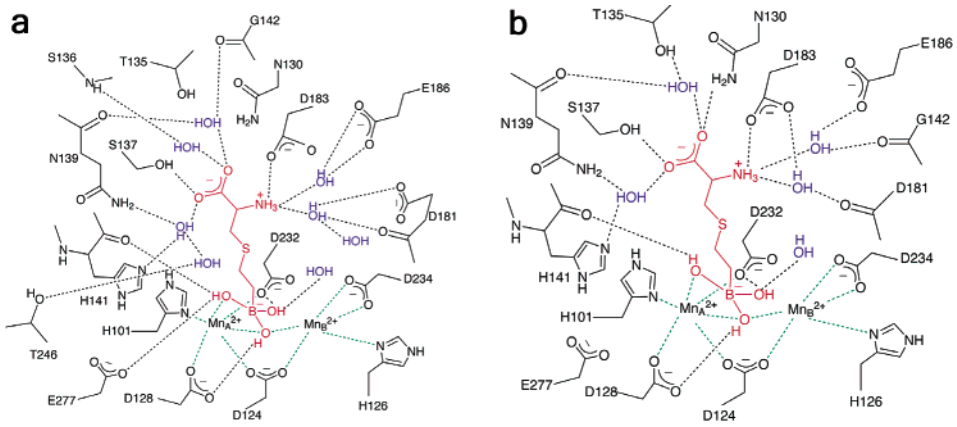

FIGURE 6: (a) Summary of intermolecular interactions in the arginase II−BEC complex. Manganese coordination interactions are designated by green dashed lines, and hydrogen bonds are indicated by black dashed lines. (b) Summary of intermolecular interactions in the arginase I−BEC complex. Manganese coordination interactions are designated by green dashed lines, and hydrogen bonds are indicated by black dashed lines.

II−BEC complex, whereas in the arginase I−BEC complex the corresponding interaction appears slightly weaker (O···O separation = 3.3 Å).

Additional differences are evident in the binding of BEC to arginases I and II. Recognition of the α-carboxylate and α-amino groups of BEC is governed by two direct hydrogen bonds and five water-mediated hydrogen bonds with arginase II residues, whereas in arginase I this recognition is governed by three direct and four water-mediated hydrogen bonds (Figure 6). That more water-mediated enzyme−inhibitor interactions are observed in the arginase II−BEC complex may be due to the larger volume of the arginase II active site cleft. Using CAST (*36*), we calculate the volume of the active site cleft of arginase II to be 554 Å^3 and that of arginase I to be 440 Å^3. The active site cleft of arginase II fits 48 water molecules, while the active site cleft of arginase I fits only 38 water molecules, so perhaps it is not surprising that an additional water-mediated enzyme−inhibitor hydrogen bond interaction is exploited in arginase II.

As proposed for arginase I (*21*), the structure of arginase II is consistent with a metal-activated hydroxide mechanism in which both $Mn^{2+}{}_A$ and $Mn^{2+}{}_B$ activate a bridging hydroxide ion for nucleophilic attack at the substrate guanidinium group. Similar chemistry may be involved in the binding of BEC to arginases I and II, in that the metal-bridging hydroxide ion may attack the trigonal planar boronic acid to yield the tetrahedral boronate anion in the arginase I−BEC complex (*6*) and the arginase II−BEC complex (Figures 6 and 7). An alternate model, in which the preformed tetrahedral boronate binds directly to the enzyme (*19*), cannot be ruled out by the present data.

Insofar that the tetrahedral boronate anion BEC mimics the tetrahedral transition state for L-arginine hydrolysis, the crystal structure of the arginase II−BEC complex provides key inferences on two features of transition state stabilization previously unobserved in arginase I complexes. First, the hydrogen bond between boronate hydroxyl O2 and E277 is consistent with the proposal that E277 hydrogen bonds with the η_1-NH_2 group of the substrate and stabilizes the tetrahedral transition state and intermediate (*21*). Second, the arginase II−BEC structure is the first to show that D232 undergoes changes in $Mn^{2+}{}_B$ coordination to hydrogen bond with boronate hydroxyl group O3; similarly, D232 could move to hydrogen bond with the η_2-NH_2 group of the substrate and tetrahedral intermediate. These changes arise primarily from the slight movement of the D232 carboxylate that aligns a syn-oriented lone electron pair directly toward boronate hydroxyl group O3. These structural insights impact the first step of arginase II catalysis as summarized in Figure 7.

Male and Female Sexual Arousal. The selectivity of inhibitors BEC and ABH toward arginase II and the lack of

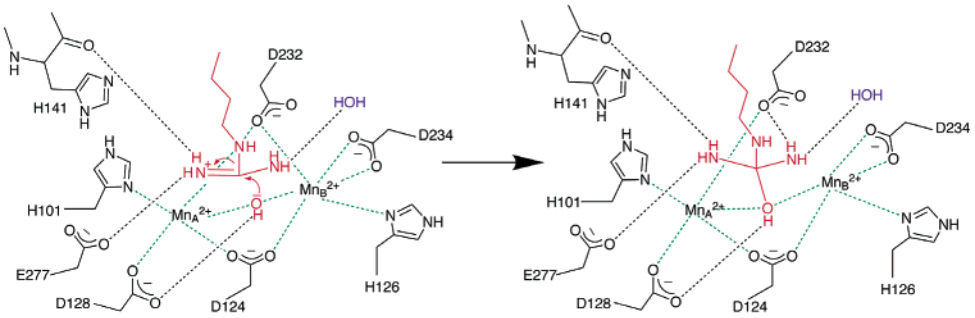

FIGURE 7: Nucleophilic attack of metal-bridging hydroxide at the substrate guanidinium group forms the tetrahedral intermediate stabilized by metal coordination and hydrogen bond interactions with D128, D232, E277, and the backbone carbonyl of H141.

activity against NO synthase (*6*, *12*) allow us to probe the role of arginase II in the regulation of NO-dependent smooth muscle relaxation in male and female genitalia. Previously, we demonstrated that both ABH and BEC enhanced relaxation of these smooth muscle tissues in ex vivo organ bath experiments (*6*, *12*). Given the selectivity of ABH and BEC, it is unlikely that these compounds bind tightly to any other cellular receptor to cause this biological effect. Inhibitors of arginase activity enhance L-arginine concentrations for NO biosynthesis and NO-dependent smooth muscle relaxation in penile corpus cavernosum, so arginase II is strongly implicated in cellular L-arginine trafficking and male erectile function. Notably, the gene expression, protein level, and catalytic activity of arginase II is elevated in diabetic corpus cavernosum, thereby implicating this isozyme in the erectile dysfunction of diabetic men (*13*).

Given the anatomical and physiological homologies between the male and the female genitalia, and given the localization of NO synthase in human clitoral corpus cavernosum (*22*) and vagina (*23*), we hypothesized that arginase II might similarly be a regulator of L-arginine bioavailability in the female genitalia, the implication being that arginase could similarly play a role in regulating female sexual arousal. To this end, conversion of L-arginine into urea was detected in extracts from rabbit vaginal tissue, indicating the presence of arginase activity. Interestingly, arginase activity was significantly higher in the distal vagina (206 nmol of urea/mg of protein) versus the proximal vagina (64 nmol of urea/mg of protein).

Given the presence of arginase activity in vaginal tissue, as well as our previous studies demonstrating the presence of arginase in penile cavernosal tissue, we investigated the effects of ABH on circulation in the genitalia of male and female rabbits in vivo. In the absence of ABH administration, pelvic nerve stimulation caused significant but submaximal increases in intracavernosal pressure and genital tissue oxyhemoglobin concentration in male and female rabbits, respectively. Repeated nerve stimulation did not result in significant changes in either parameter (data not shown). After ABH administration in male rabbits, the rise in intracavernosal pressure was not affected, but the duration of the response increased by ~28%. The overall erectile response, as reflected by the area-under-the-curve, was significantly greater with ABH (Figure 8a). Since the development of pressure within the penile cavernosal bodies is dependent upon increased arterial flow and decreased venous drainage (veno-occlusion), it is interesting to note that the amplitude of the response in male rabbits did not increase when submaximal nerve stimulation was applied

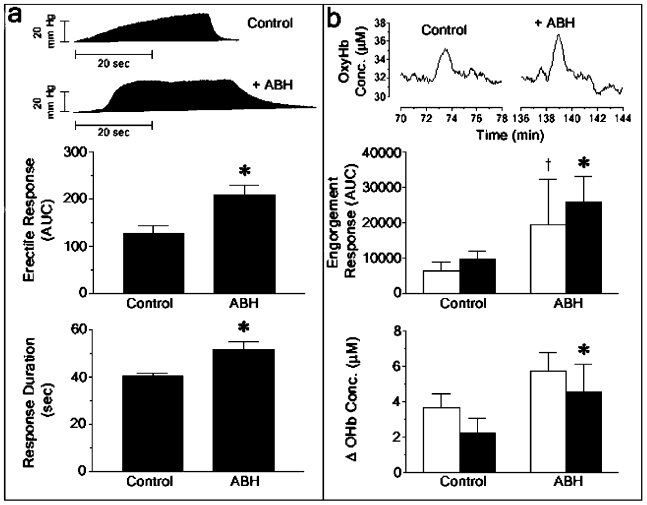

FIGURE 8: Effects of ABH administration on genital hemodynamics. For both male and female rabbits, the amplitude, duration, and area-under-the-curve (AUC) were determined for each response. All data are mean ± SEM. (a) Penile intracavernosal pressure was measured in anesthetized male rabbits to assess erectile function. The pelvic nerve was electrically stimulated 10 min after intracavernosal injection of vehicle (0.15 mL of 40% propylene glycol; control). Nerve stimulation was repeated 10 min after intracavernosal administration of ABH (150 μg). Representative recordings of intracavernosal pressure are shown in top panel. $N = 4$; $^*p < 0.05$. (b) The change in tissue oxyhemoglobin concentration (ΔOHb) was measured using near-infrared spectroscopy in anesthetized female rabbits to assess genital engorgement. The pelvic nerve was electrically stimulated 10 min after intravenous administration of vehicle (1 mL of 40% propylene glycol; control). Nerve stimulation was repeated 10 min after intravenous administration of ABH (4 or 6 mg/kg). Representative oximetry recordings are shown in the top panel. Data for rabbits that were administered the 4 mg/kg dose of ABH are shown as open bars ($N = 5$; $^*p = 0.06$ as compared to control). Data that include three additional rabbits receiving the 6 mg/kg dose of ABH are shown as solid bars ($N = 8$; $^*p < 0.05$ as compared to control).

in the presence of ABH. Thus, at the concentration tested, ABH may prolong the duration of neurogenic penile tumescence without affecting penile rigidity.

After ABH administration in female rabbits, the inhibitor consistently potentiated the rise in genital tissue oxyhemoglobin concentration triggered by pelvic nerve stimulation (Figure 8b). For the group that was administered the 4 mg/kg dose of ABH, this enhancement in genital engorgement approached statistical significance with $p = 0.06$ ($N = 5$). Importantly, the enhancement of genital engorgement reaches statistical significance ($p = 0.02$ for area-under-the-curve; $p = 0.03$ for oxyhemoglobin concentration) if all data ($N = 8$) for rabbits administered either the 4 mg/kg or the 6 mg/

kg dose of ABH are combined. Interestingly, at the doses used, the ~2-fold enhancement in mean genital tissue oxyhemoglobin resulting from ABH treatment is comparable to that resulting from treatment with sildenafil, the active ingredient of Viagra (*34*). This enhancement is consistent with the small, statistically significant increase in vaginal blood flow confirmed by laser Doppler flowmetry (*37*). These results are consistent with the fact that achieving the engorged state in female genital tissues is highly dependent on increased arterial inflow. While we did not measure perfusion within other organs, ABH administration had no discernible effect on systemic arterial blood pressure in either male or female rabbits.

CONCLUSION

The structure of human arginase II is the first of a human arginase and the first of a mammalian type II isozyme. The active site structure is consistent with a metal-activated hydroxide mechanism in catalysis, and the boronic acid inhibitors ABH and BEC (Figure 1b) are the tightest binding inhibitors known to date (*19*). The boronic acid inhibitor BEC binds as an analogue of the tetrahedral intermediate in the arginase II mechanism, and differences in the intermolecular contacts of the α-amino and α-carboxylate groups account for enhanced binding to arginase II relative to arginase I. Interestingly, the binding of BEC to arginases I and II suggests that bridging metal ligand D232 may undergo slight changes in metal coordination interaction to accommodate the binding of the tetrahedral boronate anion and by inference the tetrahedral intermediate and its flanking transition states in catalysis.

That the boronic acid inhibitor ABH enhances erectile function in live male rabbits is consistent with our previous observations using arginase inhibitors in isolated penile cavernosal tissue (*6*, *12*). Additionally, we show for the first time that an arginase inhibitor facilitates genital engorgement in the female. We conclude that arginase inhibition enhances male and female genital blood flow during sexual arousal without affecting systemic arterial blood pressure. Accordingly, arginase II is a potential drug target for the treatment of male and female sexual arousal disorders.

ACKNOWLEDGMENT

We thank the Cornell High Energy Synchrotron Source for access to the Macromolecular Diffraction at CHESS (MacCHESS) facility.

SUPPORTING INFORMATION AVAILABLE

Inhibition assay and electron density map. This material is available free of charge via the Internet at http://pubs.acs.org.

REFERENCES

1. Christianson, D. W., and Cox, J. D. (1999) *Annu. Rev. Biochem. 68*, 33−57.
2. Ash, D. E., Cox, J. D., and Christianson, D. W. (2000) in *Manganese and its Role in Biological Processes*, Vol. 37 of *Metal Ions in Biological Systems* (Sigel, A., and Sigel, H., Eds.) p 408−428, M. Dekker, New York.
3. Herzfeld, A., and Raper, S. M. (1976) *Biochem. J. 153*, 469−478.
4. Glass, R. D., and Knox, W. E. (1973) *J. Biol Chem. 248*, 5785−5789.
5. Kaysen, G. A., and Strecker, H. J. (1973) *Biochem. J. 133*, 779−788.
6. Kim, N. N., Cox, J. D., Baggio, R. F., Emig, F. A., Mistry, S., Harper, S. L., Speicher, D. W., Morris, S. M., Ash, D. E., Traish, A. M., and Christianson, D. W. (2001) *Biochemistry 40*, 2678−2688.
7. Skrzypek-Osiecka, I., Robin, Y., and Porembska, Z. (1983) *Acta Biochim. Pol. 30*, 83−92.
8. Castillo, L., Chapman, T. E., Sanchez, M., Yu, Y. M., Burke, J. F., Ajami, A. M., Vogt, J., and Young, V. R. (1993) *Proc. Natl. Acad. Sci. U.S.A. 90*, 7749−7753.
9. Castillo, L., Sanchez, M., Chapman, T. E., Ajami, A., Burke, J. F., Young, V. R. (1994) *Proc. Natl. Acad. Sci. U.S.A. 91*, 6393−6397.
10. Shi, O., Morris, S. M., Jr., Zoghbi, H., Porter, C. W., and O'Brien, W. E. (2001) *Mol. Cell. Biol. 21*, 811−813.
11. Morris, S. M., Jr. (2002) *Annu. Rev. Nutr. 22*, 87−105.
12. Cox, J. D., Kim, N. N., Traish., A. M., and Christianson, D. W. (1999) *Nat. Struct. Biol. 6*, 1043−1047.
13. Bivalaqua, T. J., Hellstrom, W. J., Kadowitz, P. J., and Champion, H. C. (2001) *Biochem. Biophys. Res. Commun. 283*, 923−927.
14. Gotoh, T., Sonoki, T., Nagasaki, A., Terada, K., Takiguchi, M., Mori, M. (1996) *FEBS Lett. 395*, 119−122.
15. Morris, S. M., Bhamidipati, D., Kepka-Lenhart, D. (1997) *Gene 193*, 157−161.
16. Colleluori, D. M., Morris, S. M., and Ash D. E. (2001) *Arch. Biochem. Biophys. 389*, 135−143.
17. Kanyo, Z. F., Chen, C. Y., Daghigh, F., Ash, D. E., and Christianson, D. W. (1992) *J. Mol. Biol. 224*, 1175−1177.
18. Cavalli, R. C., Burke, C. J., Kawamoto, S., Soprano, D. R., and Ash, D. E. (1994) *Biochemistry 33*, 10652−10657.
19. Colleluori, D. M., and Ash, D. E. (2001) *Biochemistry 40*, 9356−9362.
20. Baggio, R., Cox, J. D., Harper, L. S., Speicher, D. W., and Christianson, D. W. (1999) *Anal. Biochem. 276*, 251−253.
21. Kanyo, Z. F., Scolnick, L. R., Ash, D. E., and Christianson, D. W. (1996) *Nature 383*, 554−557.
22. Burnett, A. L., Calvin, D. C., Silver, R. I., Peppas, D. S., and Docimo, S. G. (1997) *J. Urol. 158*, 75−78.
23. Hoyle, C. H., Stones, R. W., Robson, T., Whitley, K., and Burnstock, G. (1996) *J. Anat. 188*, 633−644.
24. Baggio, R., Elbaum, D., Kanyo, Z. F., Carroll, P. J., Cavalli, R. C., Ash, D. E., and Christianson, D. W. (1997) *J. Am. Chem. Soc. 119*, 8107−8108.
25. Adamczyk, M., Johnson, D. D., and Reddy, R. E. (1999) *Tetrahedron: Asymmetry 10*, 775−781.
26. Peter, A., Smith, K., and Brown, H. (1988) *Borane Reagents*, pp 166−173, Academic Press, Inc., San Diego.
27. Matteson, D. S., and Ray, R. (1980) *J. Am. Chem. Soc. 102*, 7590−7591.
28. Kettner, C., Mersinger, L., and Knabb, R. (1990) *J. Biol. Chem. 265*, 18289−18297.
29. Otwinowski, Z., and Minor, W. (1997) *Methods Enzymol. 276*, 307−326.
30. Navaza, J. (1994) *Acta Crystallogr. A50*, 157−163.
31. Collaborative Computational Project, Number 4 (1994) *Acta Crystallogr. D50*, 760−763.
32. Jones, T. A., Zou, J.-Y., Cowan, S. W., and Kjeldgaard, M. (1991) *Acta Crystallogr. A47*, 110−119.
33. Brünger, A. T., Adams, P. D., Clore, G. M., DeLano, W. L., Gros, P., Grosse-Kunstleve, R. W., Jiang, J. S., Kuszewski, J., Nilges, M., Pannu, N. S., Read, R. J., Rice, L. M., Simonson, T., and Warren, G. L. (1998) *Acta Crystallogr. D54*, 905−921.
34. Min, K., Kim, N. N., McAuley, I., Stankowicz, M., Goldstein, I., and Traish, A. M. (2000) *Int. J. Impot. Res. 12*(*3*), S32−S39.
35. Bewley, M. C., Jeffrey, P. D., Patchett, M. L., Kanyo, Z. F., and Baker, E. N. (1999) *Structure 7*, 435−448.
36. Liang, J., Edelsbrunner, H., and Woodward, C. (1998) *Protein Sci. 7*, 1884−1897.
37. Kim, S. W., Jeong, S. J., Munarriz, R., Kim, N. N., Goldstein, I., and Traish, A. M. (2003) *Int. J. Impot. Res*., in press.

BI034340J